Proc. Natl. Acad. Sci. USA
Vol. 79, pp. 1351–1355, February 1982
Chemistry

High-resolution solid-state NMR of quadrupolar nuclei

(magic-angle spinning/nonintegral spins/second-order quadrupole interaction/rotational echoes/catalysts)

MICHAEL D. MEADOWS, KAREN A. SMITH, ROBERT A. KINSEY, T. MICHAEL ROTHGEB, ROBERT P. SKARJUNE, AND ERIC OLDFIELD

School of Chemical Sciences, University of Illinois at Urbana–Champaign, 505 South Mathews Avenue, Urbana, Illinois 61801

Communicated by H. S. Gutowsky, September 22, 1981

ABSTRACT We report the observation of high-resolution solid-state NMR spectra of ^{23}Na ($I = 3/2$), ^{27}Al ($I = 5/2$) and ^{51}V ($I = 7/2$) in various inorganic systems. We show that, contrary to popular belief, relatively high-resolution (≈10 ppm linewidth) spectra may be obtained from quadrupolar systems, in which electric quadrupole coupling constants (e^2qQ/h) are in the range ≈1–5 MHz, by means of observation of the (1/2, −1/2) spin transition. The (1/2, −1/2) transition for all nonintegral spin quadrupolar nuclei ($I = 3/2$, 5/2, 7/2, or 9/2) is only normally broadened by dipolar, chemical shift (or Knight shift) anisotropy or second-order quadrupolar effects, all of which are to a greater or lesser extent averaged under fast magic-angle sample rotation. In the case of ^{23}Na and ^{27}Al, high-resolution spectra of $^{23}NaNO_3$ (e^2qQ/h ≈300 kHz) and α-$^{27}Al_2O_3$ (e^2qQ/h ≈2–3 MHz) are presented; in the case of $^{51}V_2O_5$ (e^2qQ/h ≈800 kHz), rotational echo decays are observed due to the presence of a ≈10^3-ppm chemical shift anisotropy. The observation of high-resolution solid-state spectra of systems having spins $I = 3/2$, 5/2, and 7/2 in asymmetric environments opens up the possibility of examining about two out of three nuclei by solid-state NMR that were previously thought of as "inaccessible" due to the presence of large (a few megahertz) quadrupole coupling constants. Preliminary results for an $I = 9/2$ system, ^{93}Nb, having e^2qQ/h ≈19.5 MHz, are also reported.

During the past 20 years or so there has been considerable interest in obtaining high-resolution NMR spectra of solids (1–6). One particularly widespread technique, originally introduced by Andrew *et al.* (1, 2) and Lowe (3) for averaging of dipolar interactions, involves high-speed sample rotation at the so-called magic angle. In the past 5 years the technique has enjoyed great popularity for investigating spin $I = 1/2$ nuclei such as ^{13}C (7) and ^{31}P (8), and more recently the technique has been applied to the spin $I = 1$ nucleus deuterium (9, 10).

In the case of spin $I = 1/2$ species, considerable narrowing is achieved for spinning rates in excess of the static linebreadth. However, such rapid spinning rates are sometimes not feasible—e.g., for some ^{13}C nuclei at very high field—in which case spinning or rotational beats or echoes—i.e., well-resolved sidebands—are formed in the NMR spectrum (8–14). Such is the case, of course, for all rigid ^{2}H-labeled species (9, 10). In the case of ^{2}H, magic-angle experiments have been carried out by using synchronous sampling methods (9, 10, 13, 14), but the minute angle adjustments required for efficient averaging make it unlikely that the technique will be useful for narrowing integral spin quadrupolar powder patterns ≥200 kHz in breadth (9, 10).

The general belief, therefore, based on the work done to date, is that it is unlikely to be practical to obtain high-resolution spectra of quadrupolar nuclei in the solid state for systems having large (≈1–5 MHz) quadrupole interactions, not only for the technical reason outlined above but also because of the increasing importance of second-order quadrupole effects which increase as $(e^2qQ/h)^2$ (15, 16).

In this paper, we indicate that such problems may be circumvented to a large extent by operation at very high magnetic field strength and observation solely of the (1/2, −1/2) spin transitions of nonintegral spin quadrupolar nuclei, under conditions of magic-angle sample spinning. Because heteronuclear (e.g., ^{1}H) decoupling and enhancement also may be used in such systems, and because second-order effects in many cases may be averaged to very small values, our observations open new areas of application of the magic-angle sample-spinning technique to high-resolution NMR of solids of chemical and biological interest. Independently of this work, Müller *et al.* (17) have reported high-resolution NMR spectra of some aluminum oxide compounds, some of which exhibit broad lines in the solid state (18).

MATERIALS AND METHODS

Spectra were obtained either on a "home-built" double-resonance spectrometer (19) which now utilizes a 4.0-inch (10.2-cm)-bore 3.5-T superconducting solenoid (Nalorac Cryogenics, Concord, CA), together with a Nicolet (Madison, WI) 1280 computer system, and a home-built magic-angle sample-spinning probe which typically operates between 2.0 and 3.0 kHz or on a "home-built" 3.5-inch (8.9-cm)-bore 8.5-T superconducting solenoid (Oxford Instruments, Osney Mead, Oxford, England) based spectrometer which utilizes a Nicolet 1180/Explorer IIIC system and a second magic-angle sample-spinning probe which operates between 4 and 6 kHz. Proton decoupling was unnecessary for the spectra shown herein, but it is available. The 90° pulse widths were ≈2–3 μsec for each system studied. In most of the samples discussed, the magic angle was set by observing single-shot free induction decays on an oscilloscope. All chemicals were of reagent grade except for V_2O_5 which was technical grade from Fisher. α-Al_2O_3 was a 320-m^2/g sample from Alfa-Ventron (Danvers, MA).

RESULTS AND DISCUSSION

The first application of magic-angle sample-spinning in high-resolution solid-state NMR made by Andrew *et al.* (2) in the late 1950s did in fact involve observation of a quadrupolar nucleus, ^{23}Na, as did somewhat later experiments by Kessemeier and Norberg [^{27}Al in Al metal and AlP (20)] and Cunningham and Day [^{23}Na in NaCl (21)]. However, in each instance the nuclei in question were in highly symmetric environments, and no large quadrupolar broadenings were noted. As a result, substantial line narrowings were achieved under fast magic-angle rotation conditions, because both the small dipolar and first-order quadrupolar broadenings (20, 21) were effectively averaged. For comparison with results to be discussed in more detail later, we show in Fig. 1 a typical free induction decay (at 39.7

The publication costs of this article were defrayed in part by page charge payment. This article must therefore be hereby marked "*advertisement*" in accordance with 18 U. S. C. §1734 solely to indicate this fact.

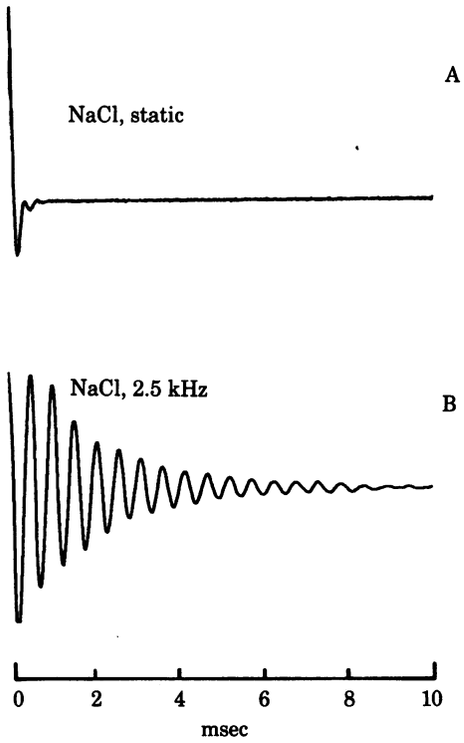

FIG. 1. ^{23}Na (I = 3/2) NMR free induction decays of polycrystalline NaCl at 39.7 MHz. (*A*) Static sample; (*B*) sample spinning at the magic angle at about 2.5 kHz.

MHz) of ^{23}NaCl, both as the static material (Fig. 1*A*) and while spinning at the magic angle at about 2.5 kHz (Fig. 1*B*). Clearly, there is a significant reduction in linewidth under magic-angle rotation, the residual width being ≈3–4 ppm.

In the presence of a large electric field gradient at the nucleus in question, as is the general case for systems of nonspherical symmetry, overall ^{23}Na spectral breadths are expected to be considerably broader than those shown in Fig. 1. For example, Pound (22) measured the electric quadrupole coupling constant of ^{23}Na in $^{23}NaNO_3$ by using single-crystal rotation techniques and obtained a value $e^2qQ/h \approx 334 \pm 2$ kHz. Presumably, the occurrence of such large quadrupole coupling constants have dissuaded many investigators from investigating such broad lines by using magic-angle sample rotation techniques.

However, Fig. 2 and Table 1 suggest why such experiments

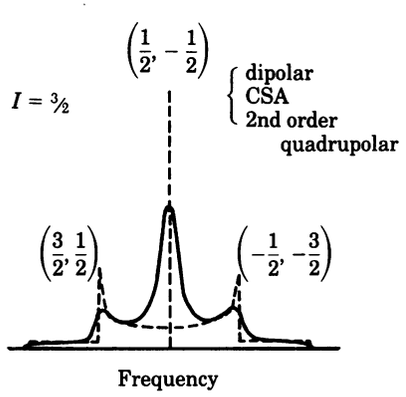

FIG. 2. Spin I = 3/2 NMR powder pattern showing that the (1/2, −1/2) transition is broadened only by second-order quadrupolar interactions, in addition to the dipolar and anisotropic magnetic shift interactions. The linewidth will thus in general be $\ll e^2qQ/h$.

could in fact be successful. As illustrated in Fig. 2, there are three transitions for the ^{23}Na nucleus: (3/2, 1/2), (1/2, −1/2), and (−1/2, −3/2). Importantly, because the central (1/2, −1/2) energy levels shift in the same way with change in sample orientation, the (1/2, −1/2) transition in general will only be broadened by dipolar, chemical shift, or Knight shift anisotropies, or by *second-order* quadrupole effects. The dipolar and anisotropic shift interactions are known to average to zero under rapid magic-angle rotation (1–3, 11, 12).

The second-order frequency shift of the central line is

$$\nu_{1/2}^{(2)} = -\frac{\nu_Q^2}{16\nu_L}(a - 3/4)(1 - \mu^2)(1 - 9\mu^2) \qquad [1]$$

in which

$$\nu_Q = \frac{3e^2qQ}{h2I(2I - 1)};\ a = I(I + 1);\ \mu = \cos\theta;$$

e^2qQ/h is the electric quadrupole coupling constant; and ν_L is the nuclear Larmor frequency.

The conventional view is that magic-angle sample-spinning experiments will be unsuccessful for most quadrupolar nuclei because the residual linebroadening is $\approx(e^2qQ/h)^2/\nu_L$. However, the detailed expression for the static second-order breadth, Eq. 1, strongly suggests that, for operation at high field (and preferably for large I), residual second-order breadths will not make the experimental spectra totally intractable. For example, we show these second-order breadths in Table 1 for three different Larmor frequencies—ν_L = 15, 35, and 100 MHz—which correspond (approximately) to the Larmor frequencies of a wide variety of quadrupolar nuclei (e.g., ^{11}B, ^{23}Na, ^{27}Al, ^{51}V, ^{55}Mn, ^{59}Co, ^{63}Cu, ^{93}Nb, etc.) at 14, 35, and 120 kilogauss. Values for spins I = 3/2, 5/2, 7/2, and 9/2 are presented.

Operation at low field and assumption of a residual second-order broadening of $\approx(e^2qQ/h)^2/\nu_L$ leads to assumption of a residual width of ≈60 kHz (Table 1) for the case of a quadrupolar nucleus having an electric quadrupole coupling constant e^2qQ/h = 1 MHz. Such a residual second-order broadening would make spectra intractable because the second-order term does not average to zero under magic-angle rotation. However, when the numerical factors in the full expression (Eq. 1) are taken into account, there is a dramatic decrease in these residual widths. For example, for the case of I = 5/2, midfield (3.5 T) operation yields a breadth of ≈900 Hz, a sizeable linewidth but significantly reduced from the 60 kHz back of the envelope calculation; at high field (12 T) the broadening amounts to only ≈3 ppm. Clearly, such residual breadths are insignificant for

Table 1. Second-order quadrupolar linewidths for spins I = 3/2, 5/2, 7/2, and 9/2 as a function of Larmor frequency

Spin I	$(e^2qQ/h)^2/\nu_L$,* Hz	$\nu_{1/2}^{(2)}$,† Hz	$\nu_{1/2}^{(2)}$,‡ ppm
3/2	≈60,000	≈3700	≈13
5/2	≈60,000	≈900	≈3
7/2	≈60,000	≈400	≈1.3
9/2	≈60,000	≈200	≈0.7

Linewidths represent either the factor $(e^2qQ/h)^2/\nu_L$ or are the maximum second-order breadth—i.e., θ = 90°, 41.8° (see Eq. 1). Sample is static.

* Approximate expression for second-order breadth, 15 MHz Larmor frequency; e^2qQ/h = 1 MHz.

† Approximate second-order breadth from Eq. 1, 35 MHz Larmor frequency; e^2qQ/h = 1 MHz.

‡ Approximate second-order breadth from Eq. 1, 100 MHz Larmor frequency; e^2qQ/h = 1 MHz.

most metal nuclei, for which chemical shift ranges of hundreds or thousands of parts per million are common. In addition, it should be noted that these widths are an upper bound because, as might be expected, there is extensive averaging of the second-order term upon rapid magic-angle rotation (for example, see refs. 1, 16, and 23 for discussion and observation of averaging of second-order broadenings by specimen rotation).

As a test of these ideas we therefore obtained magic-angle sample spinning spectra of $^{23}NaNO_3$ in the solid-state, where $|e^2qQ/h| \approx 334 \pm 2$ kHz (22). We show in Fig. 3*A* the static spectrum of $^{23}NaNO_3$ obtained using a 90° pulse width of about 2.5 μsec. Because the overall spectral breadth is $\approx$0.3 MHz (22), principally the (1/2, −1/2) transition is detected in the presence of sodium–sodium and sodium–nitrogen dipolar broadening, along with whatever small sodium chemical shift anisotropy is present, together with a small second-order quadrupole broadening term (Table 1). On magic-angle rotation at about 2.4 kHz, however, there is a long free induction decay, corresponding to a ^{23}Na linewidth of $\approx$3–4 ppm in the solid state (Fig. 3*B*). The result in Fig. 3*B* clearly shows that considerable line narrowing of the central (1/2, −1/2) transition occurs due to averaging of the relatively weak dipole–dipole (and very small CSA) interactions in this system. Averaging of such interactions is expected to be quite effective in most systems of chemical or biochemical interest, although pure metals and systems containing strong metal–metal bonds may prove to be more intractable due to strong dipole–dipole interactions. Presumably, these could be removed by suitable multiple-pulse sequences.

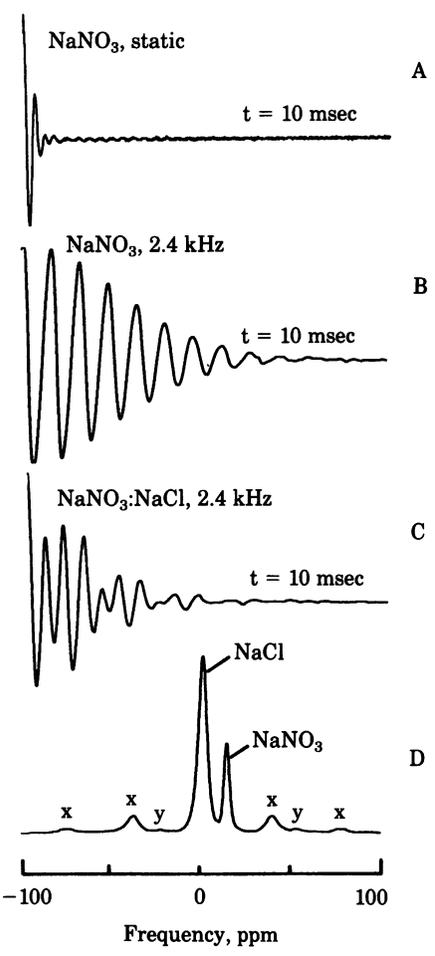

FIG. 3. ^{23}Na (I = 3/2) NMR spectra showing line-narrowing of $NaNO_3$ ($e^2qQ/h \approx$ 0.3 MHz) at 39.7 MHz. (*A*) $NaNO_3$, static free induction decay; (*B*) $NaNO_3$, free induction decay under conditions of magic-angle sample rotation at $\approx$2.4 kHz; (*C*) 1:1 molar mixture of $NaNO_3$:NaCl, free induction decay under conditions of magic-angle sample rotation at 2.4 kHz; (*D*) Fourier transform of the decay in *C*, showing high-resolution signals for both ^{23}NaCl (and side bands marked "x") and $NaNO_3$ (1/2, −1/2 transition, and side bands marked "y").

To compare more readily the linewidths and intensities of ^{23}Na in NaCl and $NaNO_3$ we show in Fig. 3*C* the free induction decay of an equimolar mixture of $^{23}NaNO_3$ and ^{23}NaCl under conditions of magic angle rotation at $\approx$2.4 kHz. Clearly, there is an interference pattern in the free induction decay due to the nonequivalent chemical shifts, and spectral intensities, of the two sodium ions. These effects are seen more clearly in the Fourier transform (Fig. 3*D*) which shows that the ^{23}NaCl resonance has a significantly increased intensity over the $^{23}NaNO_3$ resonance, due to the observation of all three transitions in the cubic phase material. The $^{23}NaNO_3$ resonance, by contrast, is considerably smaller, due primarily to the observation of predominantly the (1/2, −1/2) spin transition. The linewidths of both species are the same, $\approx$3–4 ppm.

The results of Fig. 3 were not completely unexpected because the low-field spectra of Pound (22) and the rough calculations in Table 1 indicate only a small second-order contribution to the static linewidth in the case of $^{23}NaNO_3$. By contrast, the system α-$^{27}Al_2O_3$ (corundum), also investigated by Pound (22), is known to possess a substantially larger quadrupole coupling constant, $e^2qQ/h \approx$2–3 MHz (22). We show in Fig. 4*A* the rotation pattern obtained by Pound for α-$^{27}Al_2O_3$. The curve in Fig. 4*A* follows the $(1 - \mu^2)(1 - 9\mu^2)$ rotation pattern outlined in Eq. 1 (22), indicating the presence of a large second-order quadrupole interaction. This result is not too surprising because the spectra of Fig. 4*A* were obtained by using a static magnetic field strength H_0 = 2.8 kG, in which the ^{27}Al resonance frequency is $\approx$2.6 MHz. The quadrupole interaction is therefore not a negligible fraction of the Zeeman interaction, and large second-order effects are expected. However, as pointed out above and in Table 1, such second-order effects become much smaller at high field, especially for large I (^{27}Al, I = 5/2).

We show, therefore, in Fig. 4*B* the (1/2, −1/2) transition in α-$^{27}Al_2O_3$ obtained at 35 MHz (H_0 = 35.2 kG). The linewidth is about 8.5 kHz and is comprised primarily of dipolar, second-order quadrupolar, and chemical shift anisotropy broadening. The symmetric lineshape strongly suggests that it is the dipolar interaction rather than second-order broadening that dominates the experimental spectrum, due presumably to a distribution of e^2qQ/h values in this high-surface-area sample (18). As a result, there is relatively little line narrowing upon spinning at the relatively slow speed of 2.6 kHz (Fig. 4*C*), the breadth decreasing from $\approx$8.5 to 7.0 kHz ($\approx$200 ppm). Much better resolution is obtained at higher spinning frequency with our 4- to 6-kHz probe (at 8.5 T). In addition, instrumental dead-time is also much shorter at higher operating fields and there is a reduction in the second-order term by a factor of 1/2.4. We show therefore in Fig. 4 *D* and *E* static and magic-angle spinning spectra of α-$^{27}Al_2O_3$ obtained at 93.8 MHz (corresponding to a magnetic field strength H_0 = 8.5 T). In this case the spinning frequency was $\approx$4.6 kHz, and the side bands are well resolved from the centerband (Fig. 4*E*). The reduced linewidth is $\approx$14 ppm (Fig. 4*E*), a considerable reduction from the $\approx$70 ppm static breadth for the (1/2, −1/2) transition at high field (Fig. 4*D*).

The results obtained above on ^{23}Na and ^{27}Al suggested to us that we could profitably investigate systems having even larger spins. In Fig. 5 we show spectra of V_2O_5 with and without magic-angle spinning. ^{51}V has a spin I = 7/2 and an electric quadrupole moment of about -0.4×10^{-2} barn. Previous work-

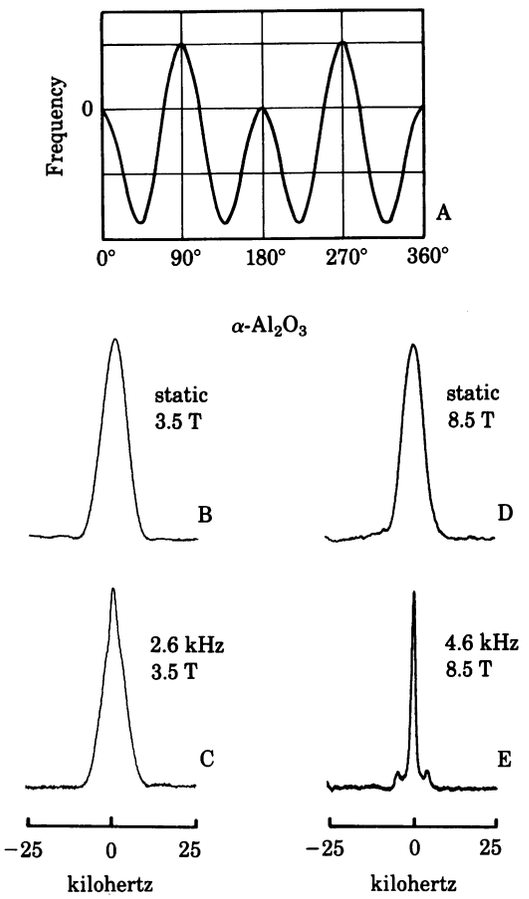

FIG. 4. ^{27}Al ($I = 5/2$) NMR spectra of α-Al_2O_3. (*A*) Rotation pattern of a single crystal of α-Al_2O_3 (corundum), after Pound (22); (*B*) 39.1-MHz Fourier transform spectrum of static sample of α-Al_2O_3; (*C*) as in *B* but under conditions of magic-angle sample rotation at ≈2.6 kHz; (*D*) 93.8-MHz Fourier transform spectrum of static sample of α-Al_2O_3; (*E*) as in *D* but under conditions of magic-angle sample rotation at ≈4.6 kHz.

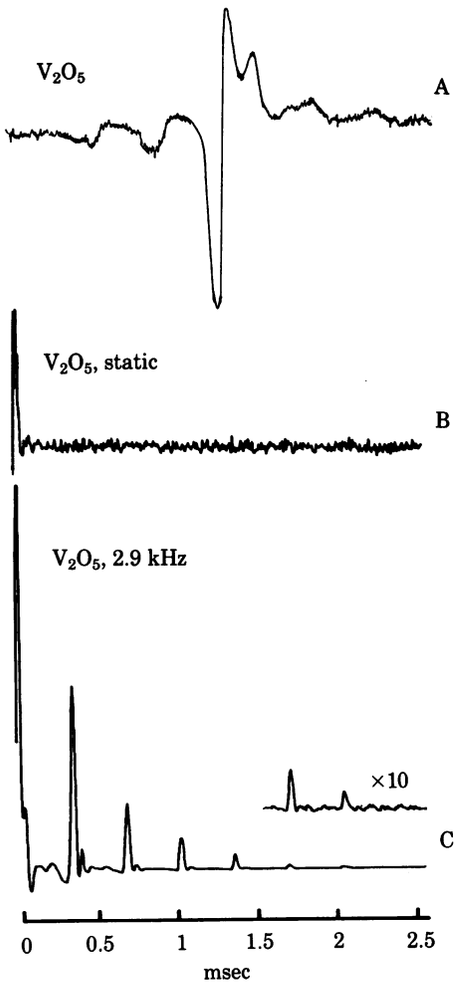

FIG. 5. ^{51}V ($I = 7/2$) NMR spectra of V_2O_5. (*A*) Static sample, wide-line derivative absorption spectrum (24); (*B*) 39.4-MHz free induction decay, static sample; (*C*) as in *B* but sample spinning at the magic angle at ≈2.9 kHz. The "rotational echoes" arise from the ≈1000-ppm chemical shift anisotropy (24).

ers (24–27) have determined the electric quadrupole coupling constant (e^2qQ/h) to be ≈800 kHz, with an asymmetry parameter (η) of ≈0.04. A typical wide-line absorption spectrum is shown in Fig. 5*A*. The free induction decay of this system when subjected to an ≈3-μsec 90° pulse is an extremely rapid transient response (Fig. 5*B*) in which we are investigating principally the central (1/2, −1/2) spin transition. On magic-angle sample rotation, large effects are again seen. Fig. 5*C* shows a typical free induction decay of $^{51}V_2O_5$ when spinning at a frequency of about 2.9 kHz. Clearly, the spectrum in Fig. 5*C* exhibits between six and seven "rotational echoes" (9, 10, 12–14). Note, however, that such responses were not observed in the case of ^{23}Na or ^{27}Al discussed above.

The reason for the presence of such echoes in the case of $^{51}V_2O_5$ may be understood by further examination of the continuous wave spectrum in Fig. 5*A*, where a splitting of the (1/2, −1/2) transition is apparent. Previous workers have determined that this originates in an ≈1000-ppm chemical shift anisotropy for the ^{51}V nucleus in this system. At 3.5 T, a 1000-ppm chemical shift anisotropy corresponds to an ≈35-kHz broadening of the central (1/2, −1/2) transition. Nevertheless, as expected, at relatively low spinning speeds most dipolar broadening is removed in this again relatively magnetically dilute lattice, and we obtain well-resolved rotational echoes because our spinning frequency (≈3 kHz) is substantially less than the anisotropy of the interaction we are averaging, the 35-kHz chemical shift anisotropy. More-rapid magic-angle spinning will naturally lead to the appearance of additional rotational echoes, opening up the possibility in some systems of synchronous sampling and two-dimensional spectroscopy of quadrupolar nuclei in solids.

Finally, we show in Fig. 6 some preliminary results on the spin $I = 9/2$ nucleus ^{93}Nb. ^{93}Nb has a 100% natural abundance, and a quadrupole moment $Q = -0.2$ barn. We chose to investigate the system $NaNbO_3$ because well-resolved second-order powder patterns have been observed for the (1/2, −1/2) transition (28). Unfortunately, however, e^2qQ/h is 19.5 MHz, because the NbO_6 octahedra are quite distorted (29, 30). Nevertheless, there is significant averaging of the second-order broadenings, with formation of a center band and associated side bands, Fig. 6, upon very rapid (≈6 kHz) spinning at high field (8.5 T, corresponding to a ^1H resonance frequency of 360 MHz).

The results discussed above now open up the possibility of examining a considerable number of quadrupolar nuclei in the solid state by using magic-angle sample spinning techniques. Contrary to popular belief, second-order quadrupole effects do not completely eliminate the possibility of obtaining high-resolution solid-state spectra for a wide variety of nuclei in the solid state. Operation at very high magnetic fields will generally be

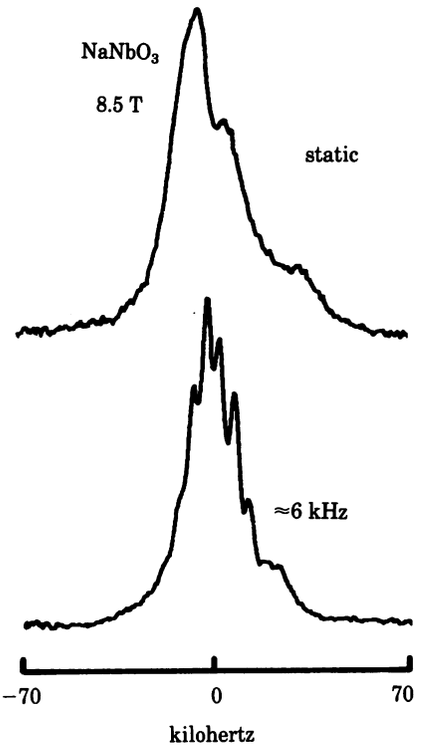

FIG. 6. $NaNbO_3$: 88 MHz ^{93}Nb ($I = 9/2$) spectra at 8.5 T. (*A*) Static sample; (*B*) sample spinning at the magic angle at ≈6 kHz. The quadrupole coupling constant for ^{93}Nb in $NaNbO_3$ is ≈19.5 MHz (28).

most advantageous, although in some cases there will be tradeoffs—for example, high-field operation affects the second-order term as H_0^{-1} while increasing the chemical shift anisotropy linearly with H_0. Therefore, correct decisions have to be made about which field strengths will be optimal, depending on the actual magnitudes of e^2qQ/h, the nuclear spin I, and the chemical shift or Knight shift anisotropy. Our results to date, however, suggest that, in general, increasing field strength will permit acquisition of spectra of higher resolution. Investigation of a wide variety of metal nuclei in systems of commercial interest—for example, catalysts and their supports, glasses and solid electrolytes—should be amenable to very high field magic-angle sample spinning techniques, as will investigation of quadrupolar nuclei such as ^{17}O, ^{25}Mg, ^{39}K, ^{43}Ca, ^{63}Cu, ^{67}Zn, and ^{95}Mo in enzymes and other biological systems.

Note Added in Proof. After communication of this article, a paper describing high-resolution NMR of ^{23}Na in solids using magic-angle spinning by Kundla *et al.* (31) appeared. Their results are consistent with ours; however, we have now found that, for systems in which second-order quadrupolar interactions are overwhelmingly dominant, that magic angles other than 54.7° are more effective in line narrowing.

Part of this work was supported by the National Institutes of Health (Grants CA-00595 and HL-19481), by the National Science Foundation (Grants PCM 78-23021 and PCM 79-23170), and by the American Heart Association (Grant 80-867) and has benefited from the use of facilities made available through the University of Illinois National Science Foundation Regional Instrumentation Facility (Grant CHE 79-16100). T.M.R. was a National Science Foundation Postdoctoral Fellow; E.O. is a U.S. Public Health Service Career Development Awardee.

1. Andrew, E. R. (1959) *Arch. Sci.* **12**, 103–108.
2. Andrew, E. R., Bradbury, A. & Eades, R. G. (1959) *Nature (London)* **183**, 1802–1803.
3. Lowe, I. J. (1959) *Phys. Rev. Lett.* **2**, 285–287.
4. Ostroff, E. D. & Waugh, J. S. (1966) *Phys. Rev. Lett.* **16**, 1097–1098.
5. Mansfield, P. & Ware, D. (1966) *Phys. Lett.* **22**, 133–135.
6. Pines, A., Gibby, M. G. & Waugh, J. S. (1973) *J. Chem. Phys.* **59**, 569–590.
7. Schaefer, J. & Stejskal, E. O. (1976) *J. Am. Chem. Soc.* **98**, 1031–1032.
8. Haberkorn, R. A., Herzfeld, J. & Griffin, R. G. (1978) *J. Am. Chem. Soc.* **100**, 1296–1298.
9. Ackerman, J. L., Eckman, R. & Pines, A. (1979) *Chem. Phys.* **42**, 423–428.
10. Eckman, R., Alla, M. & Pines, A. (1980) *J. Magn. Reson.* **41**, 440–446.
11. Andrew, E. R., Hinshaw, W. S. & Tiffen, R. S. (1974) *J. Magn. Reson.* **15**, 191–195.
12. Stejskal, E. O., Schaefer, J. & McKay, R. A. (1977) *J. Magn. Reson.* **25**, 569–573.
13. Maricq, M. & Waugh, J. S. (1977) *Chem. Phys. Lett.* **47**, 327–329.
14. Waugh, J. S., Maricq, M. M. & Cantor, R. (1978) *J. Magn. Reson.* **29**, 183–190.
15. Abragam, A. (1961) *Principles of Nuclear Magnetism* (Clarendon, Oxford), pp. 233–234.
16. Maricq, M. M. & Waugh, J. S. (1979) *J. Chem. Phys.* **70**, 3300–3316.
17. Müller, D., Gessner, W., Behrens, H.-J. & Scheler, G. (1981) *Chem. Phys. Lett.* **79**, 59–62.
18. O'Reilly, D. E. (1958) *J. Chem. Phys.* **28**, 1262–1264.
19. Oldfield, E. & Meadows, M. (1978) *J. Magn. Reson.* **31**, 327–335.
20. Kessemeier, H. & Norberg, R. E. (1967) *Phys. Rev.* **155**, 321–337.
21. Cunningham, A. C. & Day, S. M. (1966) *Phys. Rev.* **152**, 287–292.
22. Pound, R. V. (1950) *Phys. Rev.* **79**, 685–702.
23. Nolle, A. (1977) *Z. Phys. A.* **280**, 231–235.
24. France, P. W. (1980) *J. Magn. Reson.* **40**, 311–319.
25. Ragle, J. L. (1961) *J. Chem. Phys.* **35**, 753–754.
26. Gornostansky, S. D. & Stager, C. V. (1967) *J. Chem. Phys.* **46**, 4959–4962.
27. France, P. W. (1979) *J. Magn. Reson.* **34**, 585–591.
28. Wolf, F., Kline, D. & Story, H. S. (1970) *J. Chem. Phys.* **53**, 3538–3543.
29. Megaw, H. D. (1968) *Acta Crystallogr. Sect. B* **24**, 149–153.
30. Sakowski-Cowley, A. C., Kukaszewicz, K. & Megaw, H. D. (1969) *Acta Crystallogr. Sect. B* **25**, 851–865.
31. Kundla, E., Samosan, A. & Lippman, E. (1981) *Chem. Phys. Lett.* **83**, 229–232.